coatings

MDPI

Article

Mechanical Properties and Surface-Bacteria Interactions of 3D-Printed Dental Photopolymers

Senanur Aslan [1], Muhammed Turan Aslan [2,*], Çağın Bolat [2] and Ali Osman Adıgüzel [3]

[1] Faculty of Medicine, Ondokuz Mayıs University, Samsun 55270, Türkiye; senanurolfaz@gmail.com
[2] Faculty of Engineering and Natural Sciences, Samsun University, Samsun 55420, Türkiye; cagin.bolat@samsun.edu.tr
[3] Science Faculty, Ondokuz Mayıs University, Samsun 55270, Türkiye; aliosman.adiguzel@omu.edu.tr
* Correspondence: muhammedturan.aslan@samsun.edu.tr

Highlights

What are the main findings?

- Denture resin had higher strength and toughness, restoration resin had higher stiffness.
- Restoration resin showed greater wear than denture resin, though it had higher hardness.
- Optimal exposure time-depends on the resin type and the targeted mechanical or surface property.
- Both resins showed contact-mediated growth-inhibitory activity against four strains.

What are the implications of the main findings?

- Denture resin suits prosthetic bases where toughness matters more than stiffness.
- Wear in SLA resins should be assessed through surface topography, not hardness.
- Exposure time selection should be guided by the specific clinical property prioritized, not a fixed value.
- The restoration resin showed numerically higher antibacterial response across the tested strains.

Abstract

Resins printed via stereolithography are increasingly common in digital dentistry, yet the impact of production parameters on their performance remains considerable. This study examined the mechanical, tribological, and antibacterial performance of two stereolithography resins intended for restoration (white) and denture (pink) applications, selecting three different exposure times (4.5, 6, and 7.5 s) as the fabrication parameter. Compression tests showed that the white resin lost ductility with increasing exposure time, presenting statistically significant decreases in failure strain and toughness. In contrast, the pink resin maintained a stable failure strain and reached its peak energy absorption capacity at 4.5 s. Statistical analysis confirmed that the two resins responded differently to UV exposure, demonstrating that the impact of exposure time varied depending on the resin type. Furthermore, increasing exposure time significantly reduced surface roughness without a statistically significant effect on hardness. Antibacterial assessment revealed contact-mediated growth-inhibitory effects depending on strain and resin type. Accordingly, optimal exposure time was resin- and property-dependent: 7.5 s favored white resin surface quality, whereas 4.5 s maximized pink resin strength and toughness. Tailoring exposure time to both the specific resin and targeted property is crucial for enhancing the clinical longevity and structural reliability of dental applications.

Check for updates

Academic Editor: Marat R. Gafurov

Received: 27 May 2026
Revised: 22 June 2026
Accepted: 27 June 2026
Published: 30 June 2026

Copyright: © 2026 by the authors. Licensee MDPI, Basel, Switzerland. This article is an open access article distributed under the terms and conditions of the Creative Commons Attribution (CC BY) license.

Keywords: dental photopolymers; stereolithography; mechanical behaviors; friction and wear; antibacterial properties

1. Introduction

Molding and milling methods are considered standard in traditional dentistry and are widely used. However, these methods are gradually being replaced by digital manufacturing technologies, which offer high precision and a low margin of error [1,2]. Among these technologies, the computer-aided design (CAD)-integrated stereolithography (SLA) technique reduces material waste because it works on the principle of additive manufacturing [3]. The method relies on the layer-by-layer curing of liquid photopolymer resins by a computer-controlled ultraviolet (UV) laser source. This selective hardening makes it possible to produce complex anatomical geometries with micron level detail [4]. The high resolution of SLA allows a low surface roughness to be obtained in dental restorations and surgical guides and reduces the need for post-processing [5]. In personalized treatment approaches, this digital workflow adapts to the oral structure of the patient and is one of the factors that improve clinical success. However, the long-term clinical use of the method depends not only on the printing quality but also on the polymerization success of the resins used, their mechanical strength parameters, and their antibacterial behavior in interaction with the oral flora [6,7].

Dental resins used in SLA 3D-printing are typically photopolymers consisting of methacrylate- or acrylate-based monomers, oligomers, and photo initiators, and the ratio of these components directly affects the mechanical and biological properties of the final material [8]. Parameters in the printing process, particularly printing orientation, layer thickness, and post-curing processes, are critical factors that determine the performance of the produced specimens [9]. Printing orientation has a decisive effect on the mechanical properties of anisotropic materials, and it is frequently emphasized in the literature that specimens printed in a vertical orientation can exhibit different strength values due to interlayer bonding [10]. The post-curing process, on the other hand, improves both the mechanical properties and biological compatibility of the material by increasing the degree of polymerization, thereby optimizing resistance against the challenging conditions in the oral environment [11].

One of the most significant mechanical difficulties dental materials encounters in the oral environment is the compressive stress they are subjected to during chewing and biting. Therefore, sufficient compressive strength is vital for the longevity of restorations [12]. The compression test is a standard method used to evaluate the behavior of materials under compressive forces [13]. The literature reports that the compressive strength of SLA resins ranges from 20 MPa to 120 MPa, depending on the type of material and production parameters [14–18]. The effect of printing orientation on surface hardness and compressive strength has been examined in detail, particularly through the differences between 0° and 90° orientations, and it has been observed that post-curing time further improves these properties [19,20].

In addition to compressive strength, another critical mechanical property that determines the intraoral functional life of dental materials is wear resistance. Since dental restorations are in constant contact with antagonist teeth or food, they may undergo material loss over time, which can lead to a disruption of the occlusal balance [21]. Wear resistance is directly related to the surface hardness, degree of polymerization, and filler content of the material [22]. Studies show that the wear resistance of resins produced by SLA is competitive compared to those produced by traditional methods [23,24]. Never-

theless, PMMA materials produced by the milling method generally exhibit higher wear resistance due to their more homogeneous structures [25]. Nevertheless, it has been reported that the wear performance of 3D-printed resins can be significantly improved by optimizing post-curing conditions, thereby meeting clinical requirements [26].

Other than the mechanical behavior, the interaction of dental materials with the oral microbiome is also a critical factor affecting their clinical performance. Bacterial colonization of restorative surfaces is a known risk factor for secondary caries, peri-implantitis, and implant-associated infections, and pathogens such as *Staphylococcus aureus*, *Escherichia coli*, and *Klebsiella pneumoniae* pose a particular challenge in this respect [27–30]. The antimicrobial behavior of a restorative material is an essential part of its overall biological characterization. This aspect is becoming even more important as the transition from traditional prosthetics to digitally fabricated prosthetics accelerates in clinical practice. Antibacterial activity was tested on four bacterial strains selected to ensure both clinical relevance and microbiological diversity, as well as comparability with established antibacterial screening protocols for biomedical materials. *Staphylococcus aureus* and *Escherichia coli* are standard quality control strains recommended for antimicrobial susceptibility testing and ensure methodological reproducibility and direct comparability with the existing antibacterial literature on dental biomaterials [31,32]. *S. aureus* is also a leading cause of implant-associated infections, including peri-implantitis, and its ability to form biofilms on biomaterial surfaces poses a persistent clinical problem [33,34]. *Bacillus subtilis* (ATCC 6051), a Gram-positive organism with a well-characterized cell wall, has been included as a reference for thick-walled, non-resistant bacteria and provides a basis for interpreting the response observed for the more resistant *S. aureus* [35]. *Klebsiella pneumoniae* (ATCC 10031) was selected due to its clinical significance as an opportunistic nosocomial pathogen increasingly associated with implant-related infections, as well as its internal resistance mechanisms linked to its capsule and outer membrane [36,37]. This combination of two Gram-positive and two Gram-negative strains was chosen in this initial phase to characterize the intrinsic antibacterial behavior of the resins tested under controlled and reproducible conditions. The use of dentally specific oral colonizers and biofilm models is proposed as a priority for future work.

In this study, the mechanical, tribological, and antibacterial performance of SLA-printed dental resins were examined together. A restoration resin and a denture resin, which have different clinical applications, were produced with three different exposure times and evaluated under identical material and production parameters. The mechanical behavior of the specimens was determined through compression tests in terms of maximum strength, failure strain, toughness, and elastic modulus, the wear behavior was examined through dry sliding tests in terms of friction coefficient and volume loss and the surface roughness and hardness were characterized as complementary properties. The antibacterial properties were evaluated against four bacterial strains using agar well diffusion and OD_{600}-based growth kinetics methods. Examining the mechanical strength, wear resistance, and antibacterial performance together under the same resin and production conditions gives this study an original character, distinguishing it from studies in which the effect of exposure time is examined in isolation on a single property. This approach reveals that a given exposure time may improve one property while adversely affecting another. The process parameters and material selection in dental applications can thus be determined together according to the intended service condition. This provides an important advantage for clinical cases where mechanical strength and antibacterial resistance are required simultaneously.

2. Materials and Methods

2.1. Materials and Vat-Photopolymerization Printing

Commercial dental photopolymers developed for MSLA-based 3D-printing systems were used. In this study, Alias Dental Denture and Alias Dental Temp C&B resins (Dokuz Kimya, Aydın, Turkey), formulated for temporary restoration applications, were selected. These resins are indicated for various applications, including short-term crown and bridge restorations and rapid prototyping processes for removable dentures. These applications entail distinct mechanical requirements. In the literature, high stiffness and strength emerge as critical properties for 3D-printing resins intended for temporary crown–bridge applications [38]. In contrast, for denture base resins, energy absorption and toughness under masticatory loads and sudden impacts are considered more decisive parameters [8]. This study comparatively examined the extent to which commercial resins in the same category meet mechanical requirements and the effect of exposure time on this response. Based on data obtained from resin suppliers, the mechanical and physical properties that affect both manufacturing accuracy and the performance of the final product are presented in Table 1.

Table 1. Mechanical and physical properties of resins.

Properties	Standard	Materials	
		Alias Dental Denture	Alias Dental Temp C&B
Maximum Stress (MPa)	ISO 178	60	65
Elastic Modulus (GPa)	ISO 178	2.49	2.52
Elongation at Break (%)	ISO 178	5	4
Shore D	ISO 7619-1	92 D	95 D
HDT (°C)	ISO 75-1	110	105
Application	-	Denture	Restoration
Colour	-	Pink	White

The fabrication of the experimental specimens was carried out using a high-precision LCD/MSLA 3D-printing system (Photon Mono M5S Pro, Anycubic, Shenzhen, China). Sample geometries were digitally modeled via Fusion 360 CAD software (Autodesk Inc., San Francisco, CA, USA) in strict accordance with international testing standards. Accordingly, cylindrical specimens with a diameter of 10 mm and a height of 20 mm were designed for mechanical characterization, while disk-shaped specimens of the same diameter and 2 mm in thickness were generated for microbiological analyses. The resulting STL design files were processed using the Anycubic printer, which was selected for its substantial build volume (245 mm × 197 mm × 122 mm) and multi-sample throughput capacity. The literature reports that short exposure times can lead to insufficient curing, that exposure times around 6 s tend to provide optimal performance, and that longer exposure times approach the effects of over-curing [39–41]. Accordingly, in the present study, three different exposure times selected as production parameters, representing under-curing, the optimal range, and over-curing, respectively. The specific processing parameters during photopolymerization are summarized in Table 2, and the comprehensive manufacturing workflow is detailed in Figure 1. Additionally, since the bacteria–surface interaction is contact-mediated, the smoothest surface ensures the most controlled testing condition. Based on the surface roughness results obtained in the present study, the 7.5 s exposure time was identified as the condition yielding the lowest surface roughness, and all antibacterial tests were therefore conducted on disk specimens produced under this specific condition.

Table 2. LCD/MSLA manufacturing parameters.

Variables	Levels
Layer thickness (µm)	50
Light-off delay (s)	3
Building direction	Vertical
Exposure time (s)	4.5; 6; 7.5
Light speed (mm/min)	120
Retract speed (mm/min)	240
Lift distance (mm)	5–7
UV wavelength (nm)	405
Light transmittance (%)	6

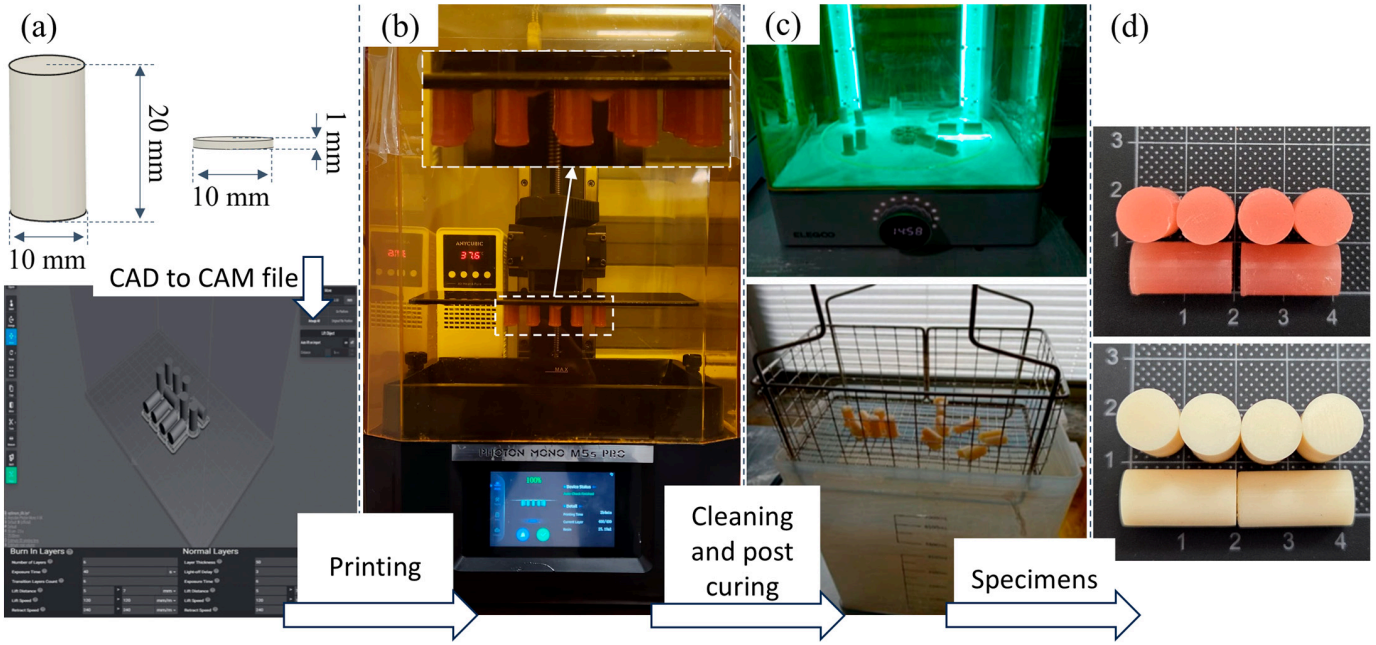

Figure 1. Step-by-step manufacturing flow diagram for dental specimens [41]; (**a**) CAD and G-Code generation, (**b**) AM process, (**c**) post- processing and (**d**) specimens (pink and white) obtained after the processes.

Following the fabrication process, the specimens were carefully detached from the build plate using a spatula. All samples underwent a thorough macroscopic inspection to detect any surface inconsistencies, such as visible stains, cracks, grooves, or deformation lines. Specimens that successfully passed the initial quality control were cleansed in a fresh isopropyl alcohol (C_3H_8O) bath to eliminate unpolymerized resin residues and micro-scale irregularities. The cleaning procedure was conducted for 10 min using an Elegoo Mercury XS (Shenzhen, China) wash-and-cure station, with the specimens secured within a specialized metal basket. Following this solvent-based purification a step widely recommended by printer manufacturers a secondary UV post-curing process was performed for 10 min within the same equipment to ensure the specimens achieved their final mechanical properties.

2.2. Mechanical and Tribological Test Setups

The durability of dental materials to the complex and continuous mechanical stresses encountered in the dynamic intraoral environment is a fundamental determinant of clinical success and restoration longevity. In this context, comprehensive compression and wear

tests were conducted to analyze the structural integrity and functional sustainability of the developed dental resins.

To evaluate the mechanical performance and volumetric compressibility of the specimens, axial compression tests were performed in accordance with ASTM D695 standards. The testing was conducted at room temperature under standard laboratory conditions using a universal testing machine (Besmak BMT-e300, Ankara, Turkey). The cylindrical specimens were vertically centered between the compression platens and loaded at a constant crosshead speed of 1 mm/min until fracture occurred. The force–displacement curves obtained from the tests were converted into engineering strain (σ)-strain (ε) curves. The stress value was calculated by dividing the applied force by the initial cross-sectional area of the specimen, and the strain was calculated by dividing the change in specimen length by the initial length. The elastic modulus (E) of the sample was determined from the slope in the elastic region of the obtained stress–strain curve using Hooke's law ($E = \sigma/\varepsilon$). In the calculation, the stress and strain values between the beginning and end of the linear region were used. The toughness, defined as the strain energy absorbed per unit volume up to failure, was determined from the area under the stress–strain curve. This area was calculated numerically by applying the trapezoidal rule to the experimentally obtained stress–strain data in MATLAB (version R2024a). Additionally, the failure strain is defined as the unit strain at the point where the specimen loses its structural integrity (formation of a macro crack or fracture) during the test. In order to ensure the consistency of the experimental data, three samples from each group were tested, and the results are reported as the mean ± standard deviation. Images of the elastic and plastic behaviors of the samples and their fracture states during testing are shown in Figure 2.

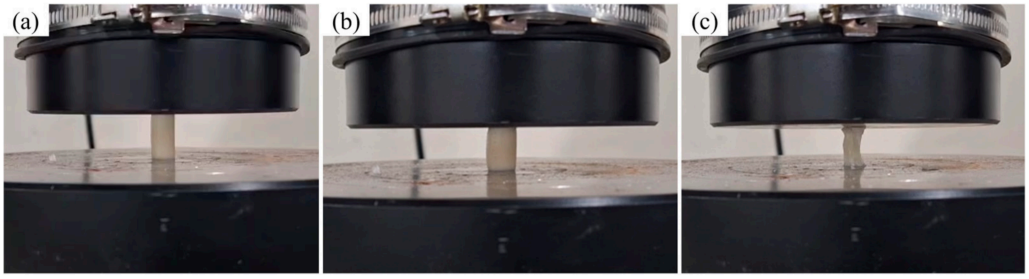

Figure 2. Stages of the axial compression test: (**a**) initial elastic state, (**b**) plastic deformation with visible bulging prior to fracture and (**c**) sample after fracture.

Hardness tests were conducted using a Shore D durometer (Loyka LX-D model, Istanbul, Turkey) to determine the surface hardness of the samples. In accordance with the ASTM D2240 standard, repeated measurements were taken on each sample, and the average of the obtained values was recorded as the hardness value for the respective sample. Using this method, the effects of different resin groups and processing conditions on surface hardness were quantitatively demonstrated.

The tribological characteristics and resistance to wear of the materials were assessed through a dry sliding pin-on-disk testing apparatus (Turkyus Podwt model wear test machine, Bursa, Turkey). These evaluations strictly adhered to the ASTM G99 standard. For the purpose of abrading the fabricated samples and measuring their wear performance, self-adhesive SiC papers, specified with 320-grit size, served as the counter-face material. To block any residual surface influence from prior deformations, a fresh counter-face paper was employed for each individual test, and a 240 m sliding distance was reached for all specimens during two minutes of deformation. All tests were carried out at room temperature and with an open-air cabinet. In addition, density values of the samples were kept identical (1.20 g/cm^3), and the mass values of the samples were measured

via a precision balance (Radwag AS 220 model; Radom, Poland) for both weight gain and loss evaluations. As for the contact surfaces, the top surfaces of the products were utilized to hinder the undesired top-and-valley structures of the bottom surfaces. To thoroughly investigate the predominant damage mechanism, a constant force magnitude of 15 N was applied during the tests. The wear experiments were executed at a consistent velocity of 2 m/s, with the friction force magnitudes precisely quantified utilizing Esit Data Logger V1.1.8 software.

Subsequently, the coefficient of friction (CoF) for each sample was derived directly from the meticulously recorded friction forces. For the comprehensive wear analyses, the methodology centered on the principle of volume loss, necessitating precise monitoring of the mass variations observed in each sample both prior to and following the experimental procedures. Consequently, the quantitative values for the coefficient of friction and the corresponding volume loss were determined by applying Equation (1) and Equation (2), respectively.

$$CoF = \frac{F}{N} \tag{1}$$

$$V_L = \frac{m_L}{\rho} \tag{2}$$

In these equations, CoF denotes the coefficient of friction, F represents the frictional force, N signifies the normal force, V_L indicates the volume loss, m_L refers to the mass loss, and ρ symbolizes the density. The experimental setup for the friction test, including both its actual and schematic representations, is presented in Figure 3.

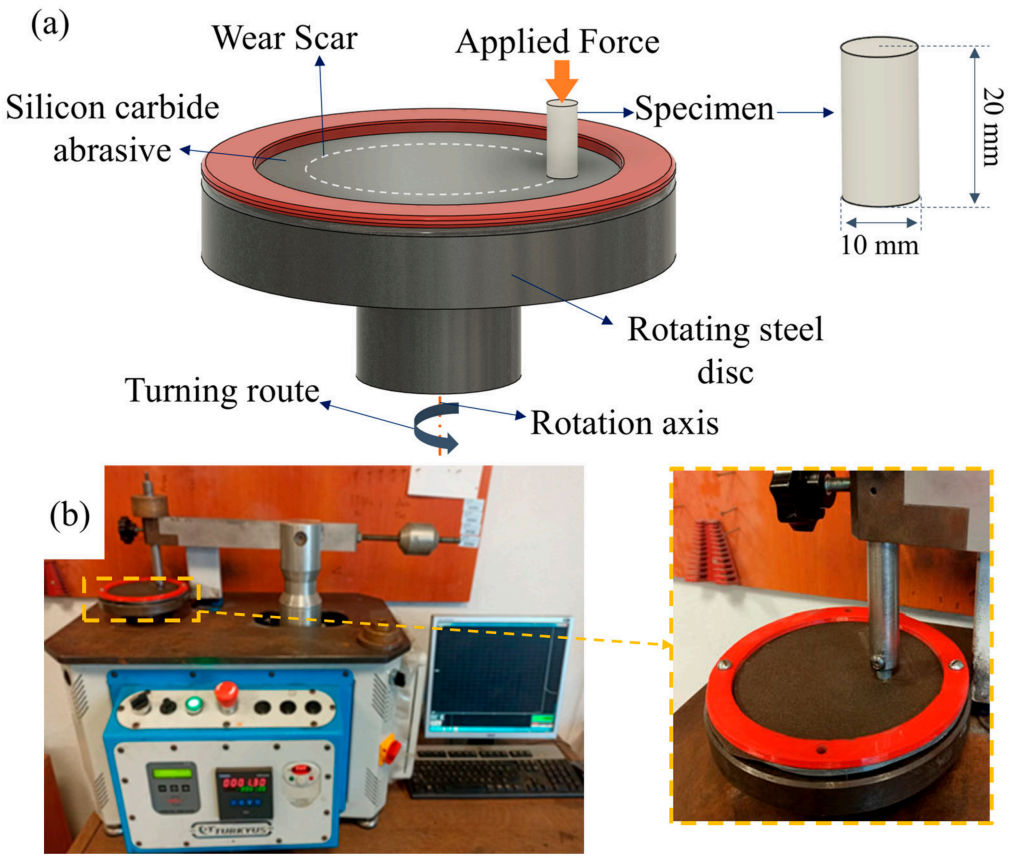

Figure 3. (**a**) Schematic view of the dry sliding test setup and (**b**) a real-time overview image showing a close-up of the deformation zone [41].

2.3. Microbiological Analyses

2.3.1. Bacterial Culture and Conditions

Four reference bacterial strains were used in this study: two Gram-positive, *Bacillus subtilis* (ATCC 6051) and *Staphylococcus aureus* (ATCC 25923), and two Gram-negative, *Escherichia coli* (ATCC 25922) and *Klebsiella pneumoniae* (ATCC 10031). All strains were originally obtained from the American Type Culture Collection (ATCC, Manassas, VA, USA) and maintained as stock cultures in the Department of Molecular Biology and Genetics, Ondokuz Mayıs University. Prior to experiments, each bacterial strain was subcultured on Mueller–Hinton Agar (MHA; Merck, Germany) and incubated at 37 °C for 24 h to ensure viability. Bacterial inocula were prepared by suspending colonies in Mueller–Hinton Broth (MHB; Merck, Germany) and adjusting turbidity to 0.5 McFarland standard (~1×10^8 CFU/mL) by spectrophotometric measurement at 625 nm (Multiscan GO, Thermo Scientific, Finland).

2.3.2. Antibacterial Activity Assessment

Agar Diffusion Assay: Since solid resin disks are unlikely to diffuse through agar due to their polymerized matrix structure, both liquid resin formulations and solid resin-fabricated disks were tested in parallel to distinguish between the diffusible antibacterial potential of the resin components and the contact-dependent activity of the cured material. The antibacterial activity of liquid resin formulations and resin-fabricated disks was evaluated by agar well and disk diffusion methods, in accordance with the general principles outlined in the Clinical and Laboratory Standards Institute (CLSI) M02 guideline. In short, 100 µL of the standardized bacterial inoculum was spread uniformly onto MHA plates using a sterile Drigalski spatula. Wells of approximately 10 mm diameter were subsequently punched into the agar using a sterile cork borer, and 50 µL of each liquid resin formulation (pink and white) was dispensed into the respective wells. Concurrently, resin-fabricated disks produced from the same formulations were placed onto the inoculated agar surface on the same plates. Sterile distilled water was used as the negative control. All plates were incubated at 37 °C for 24 h, after which inhibition zones were measured in millimeters (mm), including the diameter of the well or disk, using a digital caliper. Ciprofloxacin (25 µg/mL) (Sigma Aldrich 17850, St. Louis, MO, USA), an antibiotic effective against both Gram-negative and Gram-positive bacteria, was used as a positive control to confirm assay performance. Each assay was performed in triplicate.

Growth Kinetics Analysis (OD_{600}): To assess the time-dependent antibacterial effect of specimens, bacterial growth kinetics were monitored by optical density measurements at 600 nm (OD_{600}) over an 8 h period [35]. MHB (50 mL) was inoculated with each bacterial strain to yield an initial concentration of approximately 1×10^5 CFU/mL. In the experimental groups, resin disks (pink or white) were added to the inoculated broth prior to incubation. Control groups consisted of bacterial cultures in MHB without disks. An additional control group, consisting of sterile medium and resin disks without bacteria, was included to verify the sterilization process and assess potential optical interference from resin leachates. All cultures were incubated at 37 °C with orbital shaking at 150 rpm (Miprolab MCI-120 S, Ankara, Turkey). Samples were collected at hourly intervals and centrifuged at 10,000 *g* for 10 min. To eliminate any potential interference from environmental contaminants or impurities in the resin, the bacterial pellets were washed twice with sterile distilled water and then resuspended in an equivalent volume of distilled water prior to spectrophotometric absorbance measurements. Each condition was tested in triplicate, and

results are expressed as mean ± standard deviation. The percentage of growth inhibition at 8 h was calculated relative to the respective control group using the following Equation (3):

$$Inhibition\ (\%) = \left(1 - \frac{OD_{600_{test}}}{OD_{600_{control}}}\right) \times 100 \quad (3)$$

2.4. Statistical Analysis

A two-way analysis of variance was performed to determine the main effects of resin type and exposure time on the measured mechanical and tribological properties of the samples, as well as any potential interaction effects. Where significant main effects were identified, multiple comparisons between group means were carried out using the Tukey HSD post hoc test. The assumptions of ANOVA were verified prior to applying the analysis: the normality of residuals was tested using the Shapiro–Wilk test, and the homogeneity of variance across groups was tested using Levene's test. The variance homogeneity assumption was satisfied for all measured properties ($p > 0.05$), while the normality assumption was met for six of the eight properties; the residuals of the surface roughness ($p = 0.007$) and the hardness ($p = 0.010$) showed some deviation from normality. Given the fully balanced experimental design ($n = 3$ for each of the six conditions) and the consistent satisfaction of the variance homogeneity assumption, two-way ANOVA was applied to all variables, as the test is known to be robust to moderate deviations from normality under balanced designs. To evaluate the magnitude of the observed effects independently of sample size, p-values were reported with partial η^2 effect size values. In addition, the statistical analysis of bacterial growth kinetics data was performed using a two-way ANOVA followed by a Tukey post hoc test. The normality of residuals was verified using the Shapiro–Wilk test and was satisfied for all variables ($p > 0.05$). All statistical analyses were performed using the statsmodels package (version 0.14) in Python 3.11, and a significance level of $p < 0.05$ was adopted.

3. Results

3.1. Mechanical Results

In this study, compression tests were conducted on two distinct types of dental resins (white restorative resin and pink denture base resin) fabricated using LCD/MSLA 3D-printing technology. Specimens were produced utilizing three different exposure times: 4.5 s, 6 s, and 7.5 s. The stress–strain curves are presented separately for each resin group to show the effect of exposure time on mechanical behavior (Figure 4). These analyses highlight the critical impact of exposure time on the mechanical performance of resins employed in dental applications.

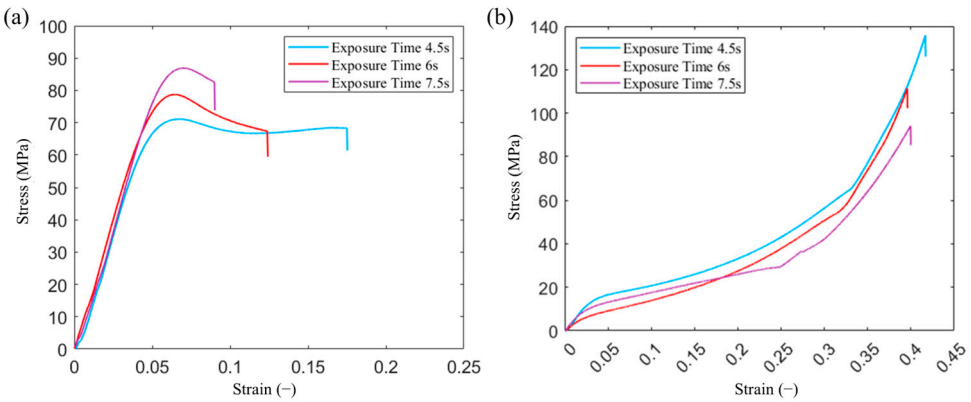

Figure 4. Stress–strain curves of (**a**) white and (**b**) pink resins.

Upon examining the stress–strain curves for the white restoration resin, the maximum stress increased steadily with the exposure time, rising from 68.86 MPa at 4.5 s to 86.92 MPa at 7.5 s. This trend was accompanied by a marked decrease in the failure strain. The simultaneous increase in strength and decrease in deformation capacity indicates that longer exposure times produced a more rigid and less ductile mechanical response in the white resin. In dental applications, restorations produced with longer exposure times may sustain higher static loads, while their tolerance to sudden impacts capable of inducing high deformation could be reduced.

Analysis of the stress–strain curves for the pink denture base resin specimens revealed that the strain values remained remarkably similar across all tested exposure times (4.5 s, 6 s, 7.5 s). This suggests that the pink resin maintained a consistent deformation capacity irrespective of the exposure time. Conversely, it was found that the stress value increased as the exposure time decreased. The behavior of these curves indicates that the pink resin exhibited higher compressive strength at shorter exposure times while preserving its deformation capability. This characteristic could be desirable in applications such as denture bases, as the material can maintain sufficient flexibility for intraoral adaptation while becoming more resistant to masticatory forces. This property of the pink resin suggests that varying exposure times modified the material's internal structure to enhance its strength without significantly compromising its deformation capacity.

The variation of the mechanical properties of the specimens produced by the LCD/MSLA method depending on the exposure time is given in Figure 5, where the polymerization behavior of the two resins is examined comparatively. The white resin increased its elastic modulus by 33.9% during the transition from 4.5 to 6 s and reached its highest value of 1.53 GPa. As the exposure time was raised to 7.5 s, the modulus declined. This result suggests that the optimum cross-linking threshold for the white resin lies around 6 s, and that a longer exposure may reduce the rigidity by inducing internal stresses in the polymer chains. It has been reported in literature studies that exposure time directly affects the mechanical strength of different photocurable resins and determines a similar stress–strain behavior [42]. The increase in rigidity of the white resin occurred together with a marked loss of ductility. As the exposure time increased from 4.5 to 7.5 s, the failure strain decreased by 54.7% and the toughness by 48.9% the failure strain decreased by 54.7% and the toughness by 48.9% (both effects statistically significant, $p < 0.001$). The reduction of the energy absorption capacity by nearly half indicates that the white resin shifts toward a glassy and brittle structure with the rising radiation energy.

The pink resin followed a different mechanical behavior from the white resin and offered a higher balance between strength and ductility. At an exposure of 4.5 s, the pink resin reached the highest maximum stress value of the study, 149.34 MPa, which exceeds the strength of the white resin at the same duration (resin effect, $p < 0.001$). As the exposure time was raised to 7.5 s, the maximum stress of the pink resin decreased to 94.08 MPa. Even after this considerable reduction, the pink resin at 7.5 s remained 19.5% stronger than the highest strength value recorded for the white resin. In terms of failure strain, the pink resin maintained a stable ductility of around 40% regardless of the exposure time and provided significantly more deformation capacity than the white resin ($p < 0.001$). This stability was also evident in the toughness values, as the toughness of the white resin dropped by 49% while the loss in the pink resin remained limited to 29.4%.

The two resins exhibit clearly different mechanical characters, and this distinction becomes more pronounced as the exposure time changes. The white resin is a rigid material and reaches its highest elastic modulus at 6 s exposure time. The pink resin, on the other hand, stands out in terms of strength and toughness, and it provides its best performance at 4.5 s. As the exposure time increases, the white resin embrittles rapidly, whereas the pink

resin retains its high deformation capacity and the structural reliability associated with it. The toughness of the pink resin at 4.5 s is 18.58 MJ·m^{-3}, which is approximately 3.5 times the value of the white resin at 7.5 s (254.4% higher). This difference indicates that, in dental applications where high masticatory forces and energy damping are important, using the pink resin with low exposure times is advantageous for both the strength and the service life of the material.

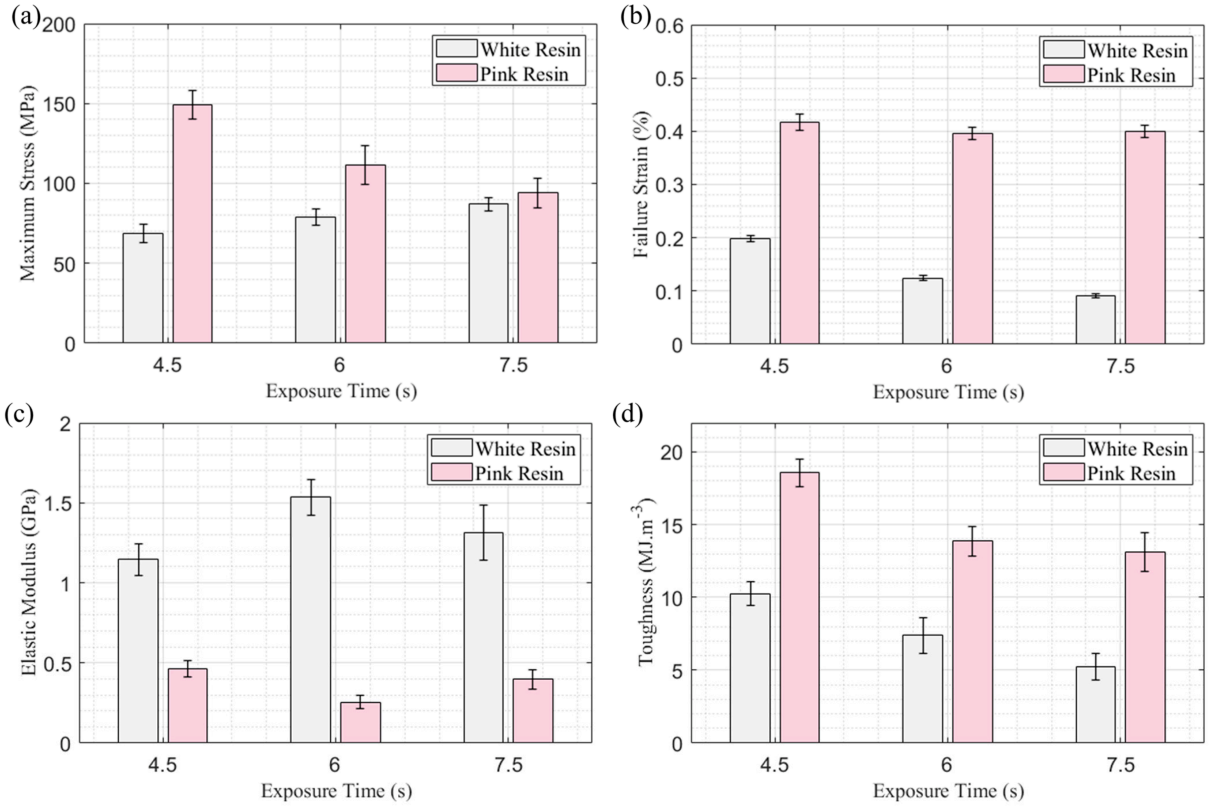

Figure 5. Comparative analysis of the (**a**) maximum stress, (**b**) failure strain, (**c**) elastic modulus, and (**d**) toughness values of MSLA resin specimens according to exposure time.

3.2. Tribological Results

3.2.1. Surface Roughness Analysis

The initial surface roughness of the printed specimens is one of the most decisive properties for the subsequent wear and friction behavior. This is because the surface quality of the starting samples may govern the deformation characteristics developing on the contact surfaces during sliding. In this work, repetitive roughness measurements were conducted using the linear deviation technique, and the mean roughness value (Ra) was used for the evaluations. The measured roughness levels of the MSLA-printed cylindrical specimens, produced from two different dental resins with three distinct exposure times, are presented comparatively in Figure 6.

Figure 6 demonstrates the measured surface roughness values (Ra) of the MSLA-printed dental specimens depending on the exposure time and resin type. At first inspection, it can be distinguished that an increasing exposure time leads to a consistent reduction in the surface roughness for both resin materials, irrespective of the resin type. According to the calculations, the lowest average roughness value of 0.41 µm (SD: 0.16) was obtained for the pink resin printed with 7.5 s exposure time. The highest level of 1.34 µm (SD: 0.14) belonged to the white resin produced with 4.5 s exposure time. Among the white resin specimens, the roughness diminished from 1.34 µm (SD: 0.14) to 0.84 µm (SD: 0.15) and 0.48 µm (SD: 0.17) as the exposure time was raised from 4.5 to 6 and 7.5 s, respectively. A parallel trend was

noted for the pink resin, where the corresponding values declined from 1.26 μm (SD: 0.15) to 0.77 μm (SD: 0.14) and 0.41 μm (SD: 0.16). Herein, the pink resin presented marginally lower roughness levels than its white counterpart for all examined exposure times.

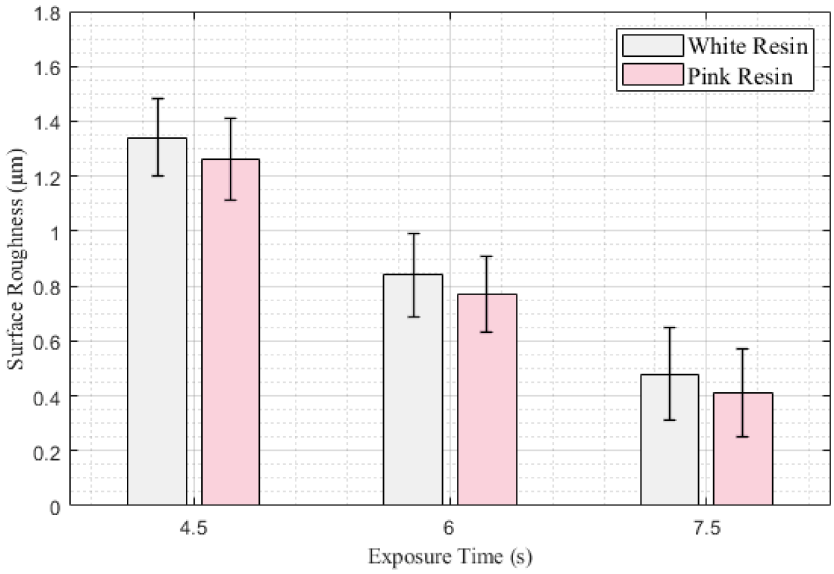

Figure 6. Values obtained from surface roughness measurements.

Regarding the effect of the exposure time, average roughness values of the samples diminish gradually for both resin types as the UV exposure is prolonged from 4.5 s up to 7.5 s. This phenomenon can be primarily attributed to the increased degree of conversion. A longer light exposure promotes a more complete monomer-to-polymer transformation within each layer and enhances the interlayer bonding. Insufficient curing durations leave partially polymerized, soft resin residues together with more pronounced layer lines on the surface, thereby elevating the R_a value. The gradual removal of these residues with prolonged exposure, in turn, provides better surface integrity. It should be noted that the reduction did not reach a plateau within the studied interval. This situation implies that the optimum curing point with respect to surface quality may lie beyond 7.5 s. Nevertheless, additional exposure times should be approached with caution since excessive curing may deteriorate the dimensional and mechanical quality of the printed parts owing to over-curing defects. When the roughness ranges reported for other resin materials tested in MSLA-based studies are examined, it is observed that the levels obtained in this study are on a similar scale and that the surface quality achieved is consistent with the ranges reported in the literature [41,43,44].

3.2.2. Hardness Results

The hardness of the tested sample is another significant factor that plays a crucial role in the friction and wear responses owing to its influence on the plastic deformation and damage characteristics. At this point, the general usage purpose of the material, the existence of abrasion during service conditions, and the mechanical requirements of the related application are decisive in the final hardness of the utilized component in terms of the designer. For dental resins, a sufficient hardness level is essential to withstand masticatory loads and abrasive contact, yet excessive hardness might bring about brittleness that limits the durability of the printed part. In Figure 7, measured Shore D hardness results of the fabricated samples can be monitored in detail depending on the resin type and exposure time.

According to the results, it was noticed that the maximum average hardness value was ascertained as 87 Shore D (SD: 3.7) for the white resin printed with 7.5 s exposure time. As

for the minimum level, an average value of 78 Shore D (SD: 4.0) was recorded for the pink resin formed with 4.5 s exposure time. Further, among the white resin samples, the average hardness value escalated from 81 Shore D (SD: 4.1) to 86 Shore D (SD: 4.8) depending on the rising exposure time. On the other hand, the pink resin reflected a different behavior, as its hardness increased from 78 Shore D (SD: 4.0) to 82 Shore D (SD: 3.2) at 6 s but then declined to 80 Shore D (SD: 4.7) at 7.5 s. As shown in Figure 7, the hardness generally tends to increase with the exposure time, although the pink resin deviates from this pattern at 7.5 s. This indicates that medium-to-high-level hardness values can be obtained for the dental resins directly after the LCD/MSLA printing. For dentistry applications such as temporary dental applications, matching the proposed LCD/MSLA process parameters with a suitable resin type offers a practical processing route.

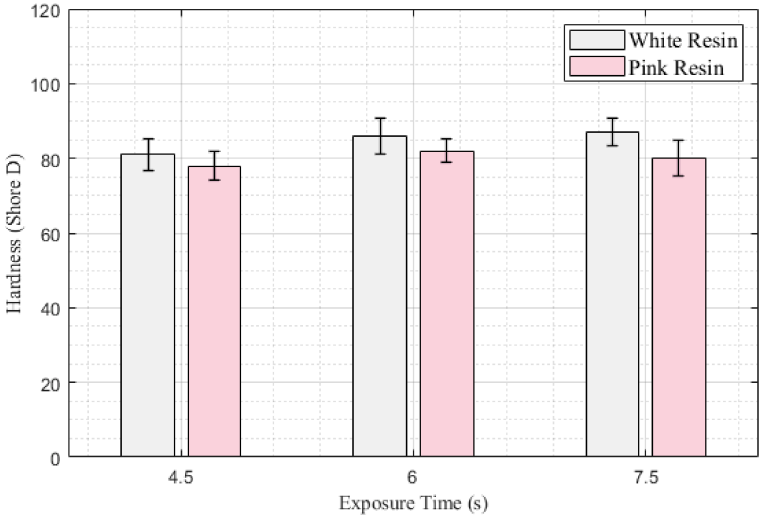

Figure 7. Hardness results of MSLA-printed samples depending on exposure time and resin material.

When the influence of the exposure time is evaluated, the prolonged exposure time generally tends to enhance the hardness, and this tendency is primarily attributed to the increase in the degree of conversion that promotes a more complete monomer to polymer transformation along with a higher crosslinking density. It has also been reported in previous studies that the process parameters significantly affect the mechanical and surface properties of MSLA-produced resins [45,46]. Nevertheless, the hardness increment of the white resin remained limited to a single unit between 6 and 7.5 s, which indicates that a plateau region is approached and the polymerization is largely completed within this interval. The slight hardness decrement noticed for the pink resin at 7.5 s might be associated with internal stresses and embrittlement stemming from excessive UV exposure, although this drop falls within the standard deviation range and should therefore be interpreted with caution. When the influence of the resin type is assessed, the white resin shows higher hardness than the pink one at all exposure times, with the numerical difference between the two materials ranging from 3 to 7 Shore D units with the rising exposure time. This tendency can be attributed to elastic modulus and rigidity shared in Figure 5c. Furthermore, it has been emphasized in the literature that the resin formulation and pigment content are decisive factors in the final hardness of dental resins [46,47].

3.2.3. Friction and Wear Behavior

The friction and wear behavior comprises the tribological properties that determine the service lifespan and operational reliability of the fabricated samples. In this study, both properties were measured using a dry sliding test setup. The friction coefficient was calculated from the ratio of the friction force recorded during contact to the applied normal

load, while the volume loss was determined from the amount of wear formed on the samples after the test.

The friction coefficient results depending on the resin type and exposure time are given in Figure 8. The two resins followed different trends here. For the white resin, the friction coefficient was 0.41 (SD: 0.014) at 4.5 s, rose to 0.47 (SD: 0.011) at 6 s, and decreased to 0.42 (SD: 0.012) at 7.5 s. For the pink resin, the trend was monotonic, as the friction coefficient increased gradually from 0.30 (SD: 0.011) to 0.33 (SD: 0.014) and then to 0.37 (SD: 0.013). The friction coefficient of the pink resin remained lower than that of the white resin at all three exposure times. The two-way ANOVA confirmed that the difference between the resins and the peak observed for the white resin at 6 s were statistically significant (resin and exposure time effects both $p < 0.001$, interaction $p < 0.001$).

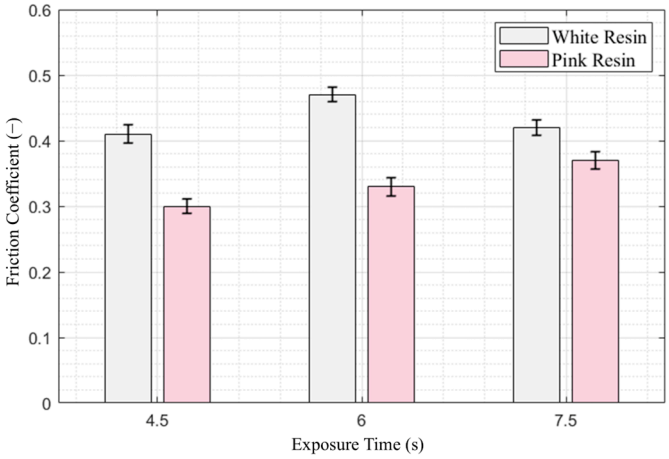

Figure 8. Friction coefficient results for MSLA-printed parts based on exposure time.

The highest volume loss was numerically obtained at 6 s exposure time for both resins. For the white resin, the volume loss rose from 121 mm^3 (SD: 5.1) to 134 mm^3 (SD: 5.4) at 6 s and dropped to 124 mm^3 (SD: 8.5) at 7.5 s. The same trend was repeated within a narrower range for the pink resin, where the volume loss increased from 116 mm^3 (SD: 7.5) to 124 mm^3 (SD: 7.1) and then decreased to 118 mm^3 (SD: 7.9). The pink resin wore less than the white resin under all three conditions. This difference reached its highest level of 10 mm^3 at 6 s. At 4.5 s, the difference decreased to 5 mm^3 and fell within the standard deviation range.

A combined assessment of the volume loss trends in Figure 9 and the friction coefficient results shows a similar trend for the white resin, where both parameters reached their highest numerical values at 6 s exposure time. A higher friction coefficient is generally associated with more energy dissipation and more severe material deformation on the contact surface, which can enlarge the volume loss. For the white resin, 6 s corresponds to an intermediate condition where the surface roughness had not yet decreased to the 7.5 s level. A still relatively rough surface may establish a more aggressive contact with the counterpart and increase the abrasive wear. Extending the exposure time to 7.5 s considerably decreases the surface roughness, and both the friction coefficient and the volume loss decline again for the white resin. The pink resin, however, displayed a different friction behavior with a monotonic increase across the tested exposure times, while still showing the highest volume loss at 6 s.

Regarding the influence of the resin type, the pink resin yielded a significantly lower friction coefficient ($p < 0.001$) and a numerically lower volume loss at all exposure times. The white resin wore more despite being harder. Given that wear is classically expected to be inversely proportional to hardness, this result indicates that wear in the present system

is governed by the surface topography and the friction behavior rather than the hardness. Indeed, it has been previously reported that the initial surface roughness regulates the wear process by influencing the contact conditions and the friction behavior [48]. When the effect of the initial surface roughness is considered in terms of the probable contact points between the surfaces, the higher average roughness of the samples having 4.5 s exposure leads to high initial plastic deformation, but as the sliding distance increases, average volume loss decreases depending on the contact surface matching change (polymer–carbide to polymer–polymer). The wear tracks and ploughing zones given with SEM (Zeiss, Gemini Model, Oberkochen, Germany) evaluations (Figure 10) support this idea for the samples having the lowest and highest volume loss results. The lower friction coefficient of the pink resin most probably originates from its smoother surface and from the contact character associated with rapid softening effect due to the escalating friction heat. In addition, the high deformation capacity of the pink resin allows it to dissipate energy through deformation rather than through brittle detachment during sliding, thereby limiting the volume loss.

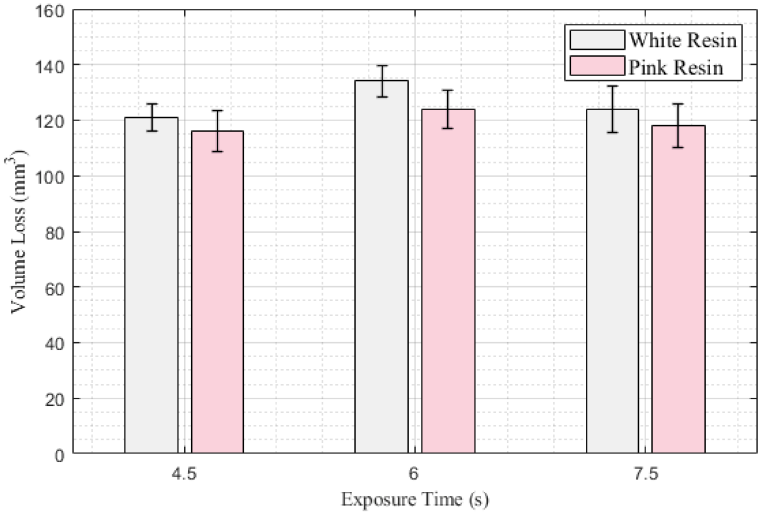

Figure 9. Volume loss results for MSLA-printed samples produced with different resins, as a function of exposure time.

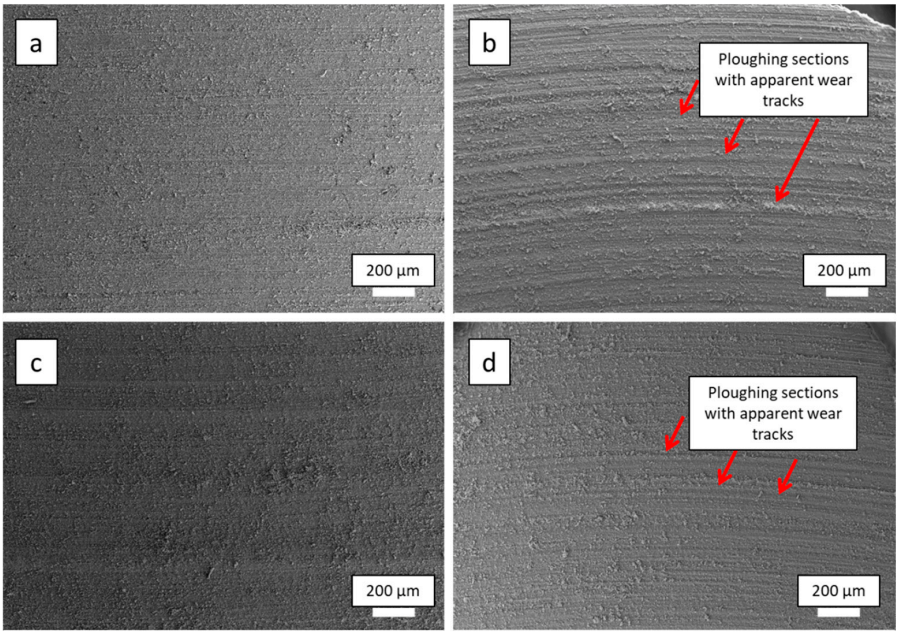

Figure 10. SEM images of the highest and lowest worn samples; white samples having 4.5 s (**a**) and 6 s (**b**) UV exposure, and pink samples having 4.5 s (**c**) and 6 s (**d**) UV exposure.

3.3. Analysis of Variance (ANOVA) and Effect Size Findings

Prior to applying ANOVA, the assumptions of normality of residuals (Shapiro–Wilk) and homogeneity of variance (Levene) were verified. The results of the two-way ANOVA for the mechanical and tribological properties examined, together with *p*-values and partial η^2 effect sizes, are presented in Table 3. The findings of the analysis of variance indicate that the independent variables did not always have a statistically significant effect on all the parameters tested. Resin type and exposure time were found to have highly significant effects on elastic modulus, toughness, maximum stress, failure strain and the coefficient of friction, whereas some main effects for surface roughness, hardness and volume loss did not reach the usual significance threshold. This situation necessitates the joint evaluation of both the numerical differences observed in the relevant properties and the effect size values.

Table 3. Two-way ANOVA for the mechanical and tribological performance of MSLA-printed dental specimens as a function of resin type and exposure time.

Property	Factor	F	*p*-Value	Partial η^2
Elastic Modulus (GPa)	Resin	422.91	<0.001	0.972
	Exposure Time	1.25	0.322	0.172
	Resin × Exposure Time	13.94	<0.001	0.699
Toughness ($MJ \cdot m^{-3}$)	Resin	227.95	<0.001	0.95
	Exposure Time	39.06	<0.001	0.867
	Resin × Exposure Time	1.24	0.324	0.171
Maximum Stress (MPa)	Resin	111.42	<0.001	0.903
	Exposure Time	8.82	0.004	0.595
	Resin × Exposure Time	32.37	<0.001	0.844
Failure Strain	Resin	3136.03	<0.001	0.996
	Exposure Time	66.55	<0.001	0.917
	Resin × Exposure Time	29.2	<0.001	0.83
Surface Roughness (μm)	Resin	1.57	0.234	0.116
	Exposure Time	46.48	<0.001	0.886
	Resin × Exposure Time	0.01	0.988	0.002
Hardness (Shore D)	Resin	5.4	0.039	0.31
	Exposure Time	1.81	0.206	0.232
	Resin × Exposure Time	0.29	0.755	0.046
Friction Coefficient	Resin	247.56	<0.001	0.954
	Exposure Time	19.31	<0.001	0.763
	Resin × Exposure Time	15.06	<0.001	0.715
Volume Loss (mm^3)	Resin	4.4	0.058	0.268
	Exposure Time	3.13	0.08	0.343
	Resin × Exposure Time	0.19	0.826	0.031

Considering the mechanical properties and coefficient of friction, it is evident that the type of resin is the key factor. The resin effect was found to be highly significant for the elastic modulus, toughness, maximum stress, fracture strain, and coefficient of friction (all $p < 0.001$), with partial η^2 values remaining above 0.90 in most cases. This finding provides strong statistical support for the hypothesis that the two resins exhibit fundamentally different mechanical and tribological behaviors. In addition, the resin and exposure time interaction effects shown in Table 3 were found to be significant for the modulus of elasticity, maximum stress, failure strain and friction coefficient, indicating that the two resins responded differently to increasing exposure times.

Exposure time had the strongest effect on surface roughness ($F = 46.48$, $p < 0.001$, partial $\eta^2 = 0.886$), and also made a significant contribution to the coefficient of friction, toughness, maximum stress and failure strain. In contrast, resin type did not result in a significant difference in surface roughness ($p = 0.234$, partial $\eta^2 = 0.116$). This result indicates that the small numerical difference observed between the two resins is not statistically significant.

The ANOVA values for the effect of exposure time on hardness and the effects of resin type and exposure time on volume loss did not reach the significance threshold. The effect of exposure time on hardness ($p = 0.206$, partial $\eta^2 = 0.232$) and the effects of resin type ($p = 0.058$, partial $\eta^2 = 0.268$) and exposure time ($p = 0.080$, partial $\eta^2 = 0.343$) on volume loss remained above the acceptable threshold. However, these partial η^2 values fall within the large effect' category according to Cohen's criteria and indicate that the underlying physical effects are of significant magnitude.

3.4. Biofouling Resistance of 3D-Printed Disks

3.4.1. Antibacterial Activity of Liquid Resin Formulations and Resin-Fabricated Disks: Agar Well and Disk Diffusion Assay

Since polymerized resin matrices are not expected to release sufficient amounts of soluble components to generate inhibition zones comparable to their unpolymerized forms [49,50], we evaluated both liquid resin formulations and solid resin-fabricated disks in parallel. This approach allowed us to differentiate between the antibacterial effects driven by diffusible components and those arising from direct surface contact of the cured material. The antibacterial activity of liquid pink and white resin formulations, along with their corresponding solid resin-fabricated disks, was assessed against *B. subtilis*, *S. aureus*, *E. coli*, and *K. pneumoniae* using the agar diffusion method. The agar diffusion results for the pink resin and white resin are presented in Figures 11 and 12, respectively, and the corresponding inhibition zone diameters are summarized in Table 4.

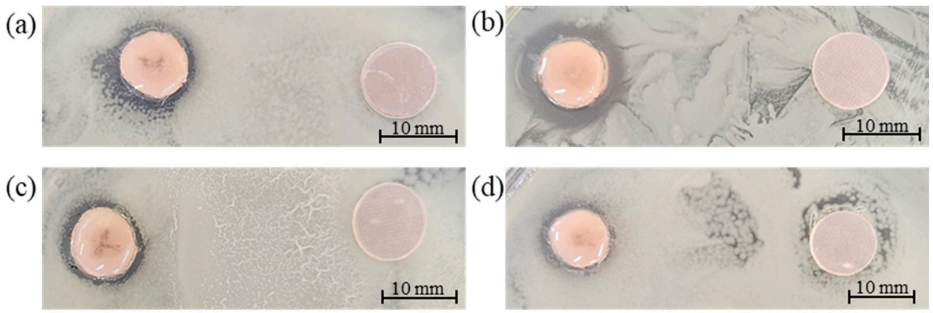

Figure 11. Inhibition zones observed following agar well and disk diffusion assays demonstrating the antimicrobial activity of liquid pink resin and pink resin-fabricated disks against (**a**) *B. subtilis* ATCC 6051, (**b**) *S. aureus* ATCC 25923, (**c**) *K. pneumoniae* ATCC 10031, and (**d**) *E. coli* ATCC 25922. In each panel, the left well contains the liquid resin formulation and the right disk represents the polymerized solid specimen.

Table 4. Inhibition zone diameters (mm) of liquid resin formulations against tested bacterial strains.

Bacterial Strain	Pink Resin Liquid (mm)	White Resin Liquid (mm)
B. subtilis	14	30
S. aureus	16	25
K. pneumoniae	12	28
E. coli	11	20

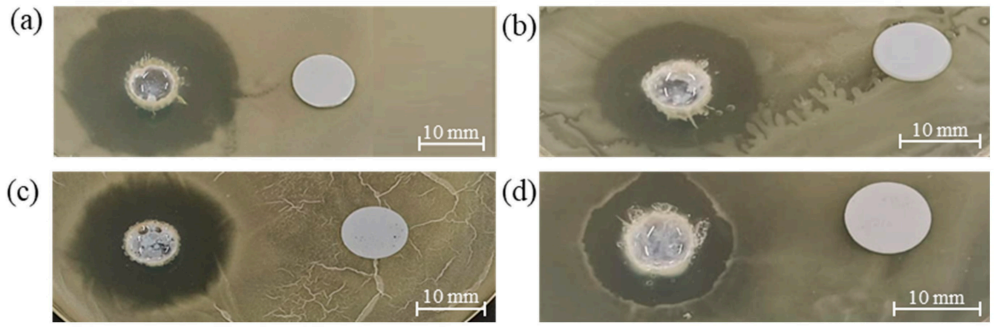

Figure 12. Inhibition zones observed following agar well and disk diffusion assays demonstrating the antimicrobial activity of liquid white resin and white resin-fabricated disks against (**a**) *B. subtilis* ATCC 6051, (**b**) *S. aureus* ATCC 25923, (**c**) *K. pneumoniae* ATCC 10031, and (**d**) *E. coli* ATCC 25922. In each panel, the left well contains the liquid resin formulation and the right disk represents the polymerized solid specimen.

Both liquid resin formulations produced measurable inhibition zones around the wells, whereas solid resin-fabricated disks did not form measurable zones against any of the tested strains. For the liquid pink resin, the largest inhibition zone was recorded against *S. aureus* (16 mm), followed by *B. subtilis* (14 mm). Reduced susceptibility was observed among Gram-negative strains, with inhibition zones of 12 mm and 11 mm for *K. pneumoniae* and *E. coli*, respectively. This differential susceptibility between Gram-positive and Gram-negative strains is attributed to the outer membrane of Gram-negative bacteria containing lipopolysaccharide (LPS) [51,52]. The liquid white resin exhibited noticeably higher antibacterial activity against all strains compared to the pink resin. *B. subtilis* showed the highest susceptibility to the white resin, with an inhibition zone of approximately 30 mm. The inhibition zones for *K. pneumoniae*, *S. aureus*, and *E. coli* were approximately 28, 25, and 20 mm, respectively. The inhibition zones caused by ciprofloxacin, used as a positive control for *B. subtilis*, *S. aureus*, *K. pneumoniae*, and *E. coli*, were 15 mm, 24 mm, 20 mm, and 42 mm, respectively (Supplementary Figure S1).

3.4.2. Time-Dependent Antibacterial Activity of Resin-Fabricated Disks: Growth Kinetics Analysis

The time-dependent antibacterial effect of the pink and white resin-fabricated disks was evaluated by monitoring bacterial growth kinetics via OD_{600} measurements at hourly intervals over an 8 h period. Growth curves for all four strains in the presence and absence of resin disks are presented in Figure 13. In all experimental groups, bacterial growth continued throughout the incubation period. However, the slope of the exponential growth phase was consistently reduced in disk containing cultures compared to controls, with no apparent prolongation of the lag phase.

For *B. subtilis* ATCC 6051, the control group reached an OD_{600} of 1.061 ± 0.049 at 8 h incubation. In comparison, bacterial growth decreased to 0.945 ± 0.045 in the presence of the pink disks and to 0.899 ± 0.006 with the white disks, corresponding to growth inhibition levels of approximately 11% and 15%, respectively. A similar trend was observed for *S. aureus* ATCC 25923, where control cultures reached 1.107 ± 0.015, compared to 0.940 ± 0.027 (~15% inhibition) and 0.928 ± 0.029 (~16% inhibition) for the pink and white disks. Among Gram-negative strains, *K. pneumoniae* ATCC 10031 control cultures attained an OD_{600} of 1.240 ± 0.085 at 8 h; the presence of the pink disks resulted in a value of 1.161 ± 0.010 (~6% inhibition), whereas the white disks reduced growth to 1.010 ± 0.042 (~19% inhibition). The most pronounced inhibitory effect among all tested strains was observed for *E. coli* ATCC 25922 in the presence of the pink disks, with an OD_{600} of 0.885 ± 0.017 (~25% inhibition) compared to a control value of 1.194 ± 0.073. The white

disks yielded an OD_{600} of 0.936 ± 0.020 (~22% inhibition) for the same strain. All results are summarized in Table 5. Growth inhibition (%) was calculated relative to the untreated control at 8 h. Control experiments conducted using sterile medium with resin disks confirmed that the absence of time-dependent changes in OD_{600} values indicated that the increase in turbidity was due solely to bacterial growth and was not influenced by optical interference from the resin disks. The consistency of this pattern across all four strains supports a growth-inhibitory mechanism for both disk formulations. In conclusion, the reduction in OD_{600} values of bacterial cultures indicates a clear growth suppression in the presence of the disk resins. However, as OD_{600} measures total biomass including both viable and non-viable cells, these results are consistent with an inhibitory effect rather than providing definitive proof of a growth-inhibitory mechanism. Therefore, further research is needed to assess the mechanism.

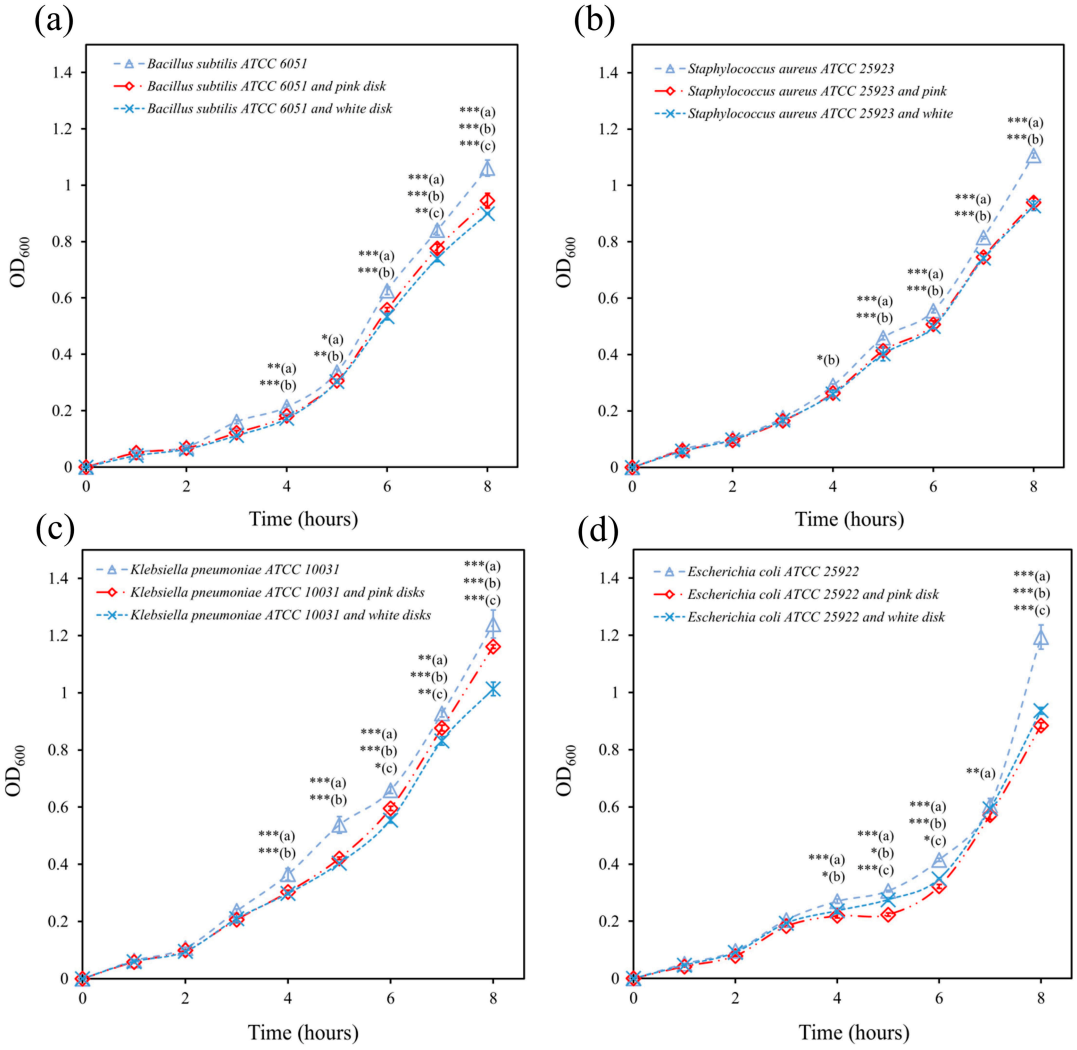

Figure 13. Growth curves (0–8 h) obtained by OD_{600} measurements of (**a**) *B. subtilis* ATCC 6051, (**b**) *S. aureus* ATCC 25923, (**c**) *K. pneumoniae* ATCC 10031, (**d**) *E. coli* ATCC 25922 strains in control, white disk, and pink disk groups within MHB medium. OD_{600} values represent the mean ± standard error of three independent replicates. Statistical significance was determined by two-way ANOVA followed by Tukey's post hoc test. (**a**) Control vs. pink disk, (**b**) control vs. white disk, (**c**) pink disk vs. white disk (* $p < 0.05$, ** $p < 0.01$, *** $p < 0.001$).

Dental materials in the oral environment face challenges primarily from complex bacterial biofilms protected by an extracellular polymeric substance (EPS) barrier, which confer higher resistance than that of planktonic cells [53,54]. Therefore, the growth-inhibitory ef-

fects observed in this study should be considered a preliminary assessment of the material's antibacterial potential.

Table 5. OD_{600} values and growth inhibition percentages at 8 h for bacterial strains cultured in the presence of the pink and white resin-fabricated disks compared to untreated controls. Values are expressed as mean ± standard deviation (n = 3).

Bacteria	Control OD_{600} at 8 h	Pink Resin Disk		White Resin Disk	
		OD_{600} at 8 h	Inhibition (%)	OD_{600} at 8 h	Inhibition (%)
B. subtilis	1.061 ± 0.049	0.945 ± 0.045	11	0.899 ± 0.006	15
S. aureus	1.107 ± 0.015	0.940 ± 0.027	15	0.928 ± 0.029	16
K. pneumoniae	1.240 ± 0.085	1.161 ± 0.010	6	1.010 ± 0.042	19
E. coli	1.194 ± 0.073	0.885 ± 0.017	25	0.936 ± 0.020	22

4. Discussion

The mechanical properties of dental resins produced via the LCD/MSLA method are directly related to the exposure time. The findings show that fundamental properties such as stiffness, ductility, and toughness vary depending on the exposure time. The characterization studies carried out on the white resin revealed that the elastic modulus reached its highest value at a 6 s exposure time. Although the main effect of exposure time on the elastic modulus did not reach statistical significance (p = 0.322), the significant resin and exposure time interaction (p < 0.001) confirmed that the two resins responded differently to the increasing duration. Exceeding this threshold led to a numerical decrease in the elastic modulus of the material [55]. This result is consistent with the brittle fracture behavior of the white resin, as both the failure strain and the toughness decreased significantly with the increased exposure time (p < 0.001 for both). The pink resin, in contrast, showed a balanced behavior between strength and ductility at a 4.5 s exposure time and exhibited a significantly higher maximum stress (p < 0.001) and a stable failure strain value. Under these conditions, the energy absorption capacity of the pink resin was approximately 1.81 times higher than that of the white resin. The ability of the pink resin to maintain its deformation capacity across the tested exposure times provides a mechanical advantage for denture bases, where structural reliability is critical [56]. The results indicate that 4.5 s is the optimal exposure time for the pink resin, as it maximizes strength, toughness, and failure strain simultaneously (p < 0.001 for all). In contrast, the optimal exposure time for the white resin varied depending on the mechanical property preferred within the tested range.

A combined examination of the surface roughness, hardness, and the friction and wear results reveals that the effect of exposure time is not unidirectional. An increasing exposure time significantly decreased the surface roughness (p < 0.001) and produced an ascending trend in the hardness, although the latter did not reach statistical significance (p = 0.206, partial η^2 = 0.232). However, these two properties exhibited different behaviors over the exposure time range. For the white resin, hardness increased by only one unit from 6 s to 7.5 s, while surface roughness continued to decrease from 0.84 µm to 0.48 µm over the same time interval. These results suggest that the 6 s exposure time is less favorable from a wear perspective. As the surface roughness has not yet decreased to its lowest level, a more aggressive contact is established with the counter surface, and the abrasive wear is increased. When the initial surface roughness is considered in terms of the probable contact points, the higher roughness of the specimens produced with 4.5 s exposure leads to high initial plastic deformation; however, as the sliding distance increases, the average volume loss decreases due to the transition of the contact surface from polymer–carbide to polymer–polymer. The wear tracks and ploughing zones observed in the SEM images support this interpretation for the specimens with the lowest and highest volume loss

results. The lower friction coefficient of the pink resin can be attributed to its smoother surface together with the softening behavior caused by the friction heat.

When analyzing the wear behavior at 7.5 s, the white resin with a significantly higher hardness (87 Shore D, resin effect $p = 0.039$) wore 124 mm^3, whereas the pink resin with a hardness of 80 Shore D exhibited a numerically lower volume loss of 118 mm^3, although the resin effect on the volume loss did not reach significance ($p = 0.058$). The significant resin and exposure time interactions detected for the friction coefficient, the elastic modulus, the maximum stress, and the failure strain (all $p < 0.001$) statistically confirm that the two resins respond differently to the same exposure time. Accordingly, the optimal exposure time-depends on both the resin type and the targeted property. For the white resin, 7.5 s produced the lowest surface roughness ($p < 0.001$) and a friction coefficient significantly lower than at 6 s ($p < 0.05$), while the friction coefficient peaked at 6 s. For the pink resin, the lowest friction coefficient was obtained at 4.5 s ($p < 0.05$ versus 7.5 s), whereas the surface roughness continued to decrease up to 7.5 s. The friction coefficient of the pink resin remained significantly lower than that of the white resin at all exposure times ($p < 0.001$), and although the difference in volume loss did not reach statistical significance, the pink resin numerically exhibited lower values. Taken together, for the white resin, the friction coefficient and volume loss were statistically indistinguishable between 4.5 s and 7.5 s, while surface roughness differed significantly between these conditions, indicating that the preferred tribological exposure time-depends on which property is prioritized. For the pink resin, however, the friction coefficient was significantly lower at 4.5 s than at 7.5 s, further supporting that the most suitable exposure time varies according to the targeted tribological property rather than a single fixed value.

In addition to examining mechanical properties, the study demonstrates that two available LCD/MSLA-printed dental resins exhibit measurable antibacterial activity against a clinically relevant panel of two Gram-positive and two Gram-negative bacteria, with distinct activity profiles emerging between diffusion-based and contact-dependent assays. Overall, both materials displayed a growth-inhibitory effect, as evidenced by a reduction in exponential growth rates without lag phase prolongation. This pattern is consistent with previous reports indicating that 3D-printed polymeric materials reduce bacterial proliferation without achieving complete eradication under planktonic conditions [35,50].

The antimicrobial evaluation of two LCD/MSLA-printed dental resins with different clinical applications revealed consistent antibacterial activity patterns, although the results varied considerably depending on the method used. In the agar well diffusion assay, both liquid resin formulations generated measurable inhibition zones, with the white resin exhibiting stronger antibacterial activity than the pink resin against all tested strains. Similar differences between photopolymer resin formulations have been reported previously and are generally associated with variations in residual monomer content and photo initiator composition [50,57]. Regarding bacterial susceptibility, the pink resin followed the expected trend of greater activity against Gram-positive bacteria than Gram-negative bacteria, likely due to the permeability barrier of the LPS containing outer membrane [51,52]. In contrast, the white resin showed a somewhat different pattern, with *K. pneumoniae* exhibiting a larger inhibition zone than *S. aureus*. This finding is noteworthy given the intrinsic resistance typically associated with *K. pneumoniae*, particularly due to its polysaccharide capsule and outer membrane structure [30]. One possible explanation is that certain diffusible components of the white resin may more readily penetrate bacterial porins, similar to what has been described for some low molecular weight hydrophilic antibacterial compounds [51]. However, further compositional analyses would be necessary to clarify this mechanism.

The OD_{600} growth kinetics data gave a different picture and pointed to a predominantly contact-dependent effect. Bacterial growth continued throughout the 8 h incubation

in all groups, but with a lower exponential growth rate and no prolonged lag phase. This pattern indicates a growth-inhibitory effect and matches earlier observations for unmodified photopolymer materials [35,49]. *E. coli* was the clearest case, since it gave the smallest inhibition zones in the diffusion assay yet showed the greatest growth reduction under direct contact (~22–25%). The pink resin was also far less active against *K. pneumoniae* (~6%) than the white resin (~19%). Taken together, the two assays measure different things rather than disagree. Agar diffusion depends on the release of soluble antibacterial components, whereas growth kinetics captures interactions at the material and bacteria interface over time. This is why a material with limited diffusible activity, such as the resin against *E. coli*, can still suppress growth substantially on contact. These represent distinct antibacterial mechanisms that may not correlate directly [35,58]. Overall, the observed inhibition levels (6–25%) are consistent with previously reported values for unmodified SLA-printed polymer systems [35,49]. Moreover, the pronounced material dependent differences observed for *K. pneumoniae* contribute valuable information to the still limited literature regarding the response of this organism to LCD/MSLA dental resins.

Several limitations should be considered when interpreting these findings. First, the degree of conversion and curing kinetics of the specimens were not evaluated. This limits our understanding of how the polymer network affects material behavior. Second, the experiments were conducted under planktonic conditions. These conditions do not fully reflect the behavior of biofilms, where bacteria are much more resistant to antimicrobial agents [59]. Third, monomer release analyses were not performed, which restricts the understanding of the chemical mechanisms.

Nevertheless, using both agar diffusion and growth kinetics assays provided a more comprehensive profile than a single method alone could offer. This proves that the choice of method directly changes the outcome of the antibacterial test. Across both tests, the resins showed a contact-mediated growth inhibition that changed with the bacterial strain and resin formulation. Ultimately, these results provide a useful baseline. In future studies, utilizing biofilm models and bacterial strains that better represent the oral microbiome, along with integrating chemical characterization methods such as FTIR and monomer release analyses, will clarify both the clinical relevance of the antibacterial behavior and the underlying curing and release mechanisms.

5. Conclusions

In MSLA-printed dental resins, exposure time governs mechanical strength, surface topography, and tribological behavior. Additionally, antibacterial efficacy at the selected 7.5 s condition depends strictly on resin formulation and bacterial strain. Because material responses to exposure time are non-linear, curing optimization cannot be reduced to a single parameter. Based on these exposure-dependent behaviors, the main findings are outlined below:

- The optimal exposure time-depends on the resin formulation and the desired properties. For the pink resin, an exposure time of 4.5 s is optimal for maximizing strength and toughness. Conversely, an exposure time of 6 s maximizes the elastic modulus of the white resin.
- Increasing the exposure time to 7.5 s consistently provides the lowest surface roughness for both resin formulations.
- In terms of antibacterial performance, both resins exhibited growth-inhibitory activity against the tested bacterial strains, with inhibition levels ranging from approximately 6% to 25%. Overall, the white resin exhibited a trend toward greater bacterial growth inhibition than the pink resin across most of the tested strains.

As a novelty, this study establishes a multi-criteria optimization map by demonstrating that MSLA-printed dental resins exhibit non-linear material responses to curing parameters, meaning no single exposure time can simultaneously optimize mechanical, surface, and biological properties.

Supplementary Materials: The following supporting information can be downloaded at: https://www.mdpi.com/article/10.3390/coatings16070779/s1, Figure S1: Inhibition zones formed by ciprofloxacin on *B. subtilis*.

Author Contributions: S.A. Conceptualization, writing—original draft, data analysis, experimental findings. M.T.A. Methodology, data analysis, writing—review and editing, experimental findings. Ç.B. Supervisor, writing—review and editing, data analysis, experimental findings. A.O.A. data analysis, writing—review and editing, experimental findings. All authors have read and agreed to the published version of the manuscript.

Funding: This research received no external funding.

Institutional Review Board Statement: Not applicable.

Informed Consent Statement: Not applicable.

Data Availability Statement: The data that support the findings of this work are available on request from the corresponding author.

Conflicts of Interest: The authors declare no conflicts of interest.

References

1. Bae, E.-J.; Jeong, I.-D.; Kim, W.-C.; Kim, J.-H. A Comparative Study of Additive and Subtractive Manufacturing for Dental Restorations. *J. Prosthet. Dent.* **2017**, *118*, 187–193. [CrossRef] [PubMed]
2. Revilla-León, M.; Özcan, M. Additive Manufacturing Technologies Used for Processing Polymers: Current Status and Potential Application in Prosthetic Dentistry. *J. Prosthodont.* **2019**, *28*, 146–158. [PubMed]
3. Dawood, A.; Marti, B.M.; Sauret-Jackson, V.; Darwood, A. 3D Printing in Dentistry. *Br. Dent. J.* **2015**, *219*, 521–529. [CrossRef] [PubMed]
4. Melchels, F.P.W.; Feijen, J.; Grijpma, D.W. A Review on Stereolithography and Its Applications in Biomedical Engineering. *Biomaterials* **2010**, *31*, 6121–6130. [CrossRef] [PubMed]
5. Kessler, A.; Hickel, R.; Reymus, M. 3D Printing in Dentistry-State of the Art. *Oper. Dent.* **2020**, *45*, 30–40. [CrossRef] [PubMed]
6. Lin, C.-H.; Lin, Y.-M.; Lai, Y.-L.; Lee, S.-Y. Mechanical Properties, Accuracy, and Cytotoxicity of UV-Polymerized 3D Printing Resins Composed of Bis-EMA, UDMA, and TEGDMA. *J. Prosthet. Dent.* **2020**, *123*, 349–354. [CrossRef] [PubMed]
7. Yue, J.; Zhao, P.; Gerasimov, J.Y.; Van De Lagemaat, M.; Grotenhuis, A.; Rustema-Abbing, M.; Van Der Mei, H.C.; Busscher, H.J.; Herrmann, A.; Ren, Y. 3D-Printable Antimicrobial Composite Resins. *Adv. Funct. Mater.* **2015**, *25*, 6756–6767. [CrossRef]
8. Lee, H.E.; Alauddin, M.S.; Mohd Ghazali, M.I.; Said, Z.; Mohamad Zol, S. Effect of Different Vat Polymerization Techniques on Mechanical and Biological Properties of 3D-Printed Denture Base. *Polymers* **2023**, *15*, 1463. [CrossRef] [PubMed]
9. Altarazi, A.; Haider, J.; Alhotan, A.; Silikas, N.; Devlin, H. Assessing the Physical and Mechanical Properties of 3D Printed Acrylic Material for Denture Base Application. *Dent. Mater.* **2022**, *38*, 1841–1854. [CrossRef] [PubMed]
10. Jain, S.; Sayed, M.E.; Shetty, M.; Alqahtani, S.M.; Al Wadei, M.H.D.; Gupta, S.G.; Othman, A.A.A.; Alshehri, A.H.; Alqarni, H.; Mobarki, A.H.; et al. Physical and Mechanical Properties of 3D-Printed Provisional Crowns and Fixed Dental Prosthesis Resins Compared to CAD/CAM Milled and Conventional Provisional Resins: A Systematic Review and Meta-Analysis. *Polymers* **2022**, *14*, 2691. [CrossRef] [PubMed]
11. Hassanpour, M.; Narongdej, P.; Alterman, N.; Moghtadernejad, S.; Barjasteh, E. Effects of Post-Processing Parameters on 3D-Printed Dental Appliances: A Review. *Polymers* **2024**, *16*, 2795. [CrossRef] [PubMed]
12. Yousef, A.; Abu-Elghait, M.; Rizk, M.S.; Abdel-Hamid, M.S.; Salem, S.S.; El-Sherbiny, G.M. Combatting Biofilm Formation of Klebsiella Pneumoniae and Bacillus Subtilis Clinical Strains from the Oral Cavity Using Biogenic Se-NPs: Molecular Docking Simulation and Cytotoxic Effects on HepG2 Cancer Cells. *BMC Microbiol.* **2025**, *25*, 446. [CrossRef] [PubMed]
13. Paradowska-Stolarz, A.; Wezgowiec, J.; Mikulewicz, M. Comparison of Two Chosen 3D Printing Resins Designed for Orthodontic Use: An In Vitro Study. *Materials* **2023**, *16*, 2237. [CrossRef] [PubMed]
14. Dzhondrova, I.; Liondev, I.; Taneva, I.; Bogdanov, T.; Uzunov, T.; Kirov, D. Effect of Printing Orientation and Post-Curing Time on the Mechanical Properties of 3D-Printed Denture Base Resin. *J. Funct. Biomater.* **2025**, *17*, 1. [CrossRef] [PubMed]

15. Vakiti, T.; Suranani, S.; Kuppusamy, R.R.P. Effect of Print Orientations, Layer Thicknesses, and Weathering on the Mechanical Properties, Failure Mechanism, and Service Life of 3D-Printed Photocured Resin Parts. *Polym. Eng. Sci.* **2025**, *65*, 797–815. [CrossRef]
16. Wang, E.; Yang, F.; Shen, X.; Li, Z.; Yang, X.; Zhang, X.; Peng, W. Investigation and Optimization of the Impact of Printing Orientation on Mechanical Properties of Resin Sample in the Low-Force Stereolithography Additive Manufacturing. *Materials* **2022**, *15*, 6743. [CrossRef] [PubMed]
17. Choi, Y.; Yoon, J.; Kim, J.; Lee, C.; Oh, J.; Cho, N. Development of Bisphenol-A-Glycidyl-Methacrylate- and Trimethylolpropane-Triacrylate-Based Stereolithography 3D Printing Materials. *Polymers* **2022**, *14*, 5198. [CrossRef] [PubMed]
18. Raykar, S.J.; D'Addona, D.M.; Gaikwad, P.M.; Bhosale, V.S.; Gaikwad, A.R.; Hajare, S.M.; Mali, S.M. Investigation and Analysis of Effect of Curing Process on Compressive Strength Performance of Stereolithography-Printed Components. *J. Mater. Eng. Perform.* **2023**, *32*, 9958–9967. [CrossRef]
19. Pantea, M.; Ciocoiu, R.C.; Greabu, M.; Totan, A.R.; Imre, M.; Țâncu, A.M.C.; Sfeatcu, R.; Spînu, T.C.; Ilinca, R.; Petre, A.E. Compressive and Flexural Strength of 3D-Printed and Conventional Resins Designated for Interim Fixed Dental Prostheses: An In Vitro Comparison. *Materials* **2022**, *15*, 3075. [CrossRef] [PubMed]
20. Tayeb, H.K.; Silikas, N.; Alhaddad, A.J.; Satterthwaite, J. Flexural Strength and Hardness Analysis of 3D-Printed vs. Milled Resin Composites Indicated for Definitive Crowns. *J. Funct. Biomater.* **2025**, *16*, 468. [CrossRef] [PubMed]
21. Myagmar, G.; Lee, J.H.; Ahn, J.S.; Yeo, I.S.L.; Yoon, H.I.; Han, J.S. Wear of 3D Printed and CAD/CAM Milled Interim Resin Materials after Chewing Simulation. *J. Adv. Prosthodont.* **2021**, *13*, 144–151. [CrossRef] [PubMed]
22. Elsharkawy, Y.M.M.; Mohamed, H.T.; El Saeedi, T.M.A.S.; Farahat, A.M.S. Comparative in Vitro Study on Wear Resistance and Colour Stability of 3D-Printed, Milled, and Conventional PMMA Denture Teeth. *BMC Oral Health* **2025**, *25*, 656. [CrossRef] [PubMed]
23. Park, J.M.; Ahn, J.S.; Cha, H.S.; Lee, J.H. Wear Resistance of 3D Printing Resin Material Opposing Zirconia and Metal Antagonists. *Materials* **2018**, *11*, 1043. [CrossRef] [PubMed]
24. Çiçek, Y.; Küçük, C. Wear of Interim Resin Materials Manufactured by 3D Printing and CAD/CAM Milling Following Chewing Simulation. *BMC Oral Health* **2025**, *25*, 1679. [CrossRef] [PubMed]
25. Lassila, L.; Mangoush, E.; He, J.; Vallittu, P.K.; Garoushi, S. Effect of Post-Printing Conditions on the Mechanical and Optical Properties of 3D-Printed Dental Resin. *Polymers* **2024**, *16*, 1713. [CrossRef] [PubMed]
26. Wada, J.; Wada, K.; Garoushi, S.; Shinya, A.; Wakabayashi, N.; Iwamoto, T.; Vallittu, P.K.; Lassila, L. Effect of 3D Printing System and Post-Curing Atmosphere on Micro- and Nano-Wear of Additive-Manufactured Occlusal Splint Materials. *J. Mech. Behav. Biomed. Mater.* **2023**, *142*, 105799. [CrossRef] [PubMed]
27. Cui, Z.; Wang, P.; Gao, W. Microbial Dysbiosis in Periodontitis and Peri-Implantitis: Pathogenesis, Immune Responses, and Therapeutic. *Front. Cell. Infect. Microbiol.* **2025**, *15*, 1517154. [CrossRef] [PubMed]
28. Balanger, M.; Hinet, M.; Vacher, C.; Bellaiche, N.; Charrier, J.L.; Millot, S. Osteomyelitis of the Mandible after Dental Implants in an Immunocompetent Patient. *Case Rep. Dent.* **2017**, *2017*, 9525893. [CrossRef] [PubMed]
29. da Silva Garrote, M.; Barbosa, A.A.C.; de Fátima Batista Medeiros Alves Teixeira, M.; Mendonça, E.F.; Fenelon, G.; Guedes, O.A.; Estrela, C. Severe Chronic Suppurative Osteomyelitis Following Dental Implant Placement. *Case Rep. Dent.* **2025**, *2025*, 6770915. [CrossRef] [PubMed]
30. Paczosa, M.K.; Mecsas, J. Klebsiella Pneumoniae: Going on the Offense with a Strong Defense. *Microbiol. Mol. Biol. Rev.* **2016**, *80*, 629–661. [CrossRef] [PubMed]
31. Clinical and Laboratory Standards Institute (CLSI). M02: Performance Standards for Antimicrobial Disk Suspectibility Tests. *Clin. Lab. Stand. Inst. (CLSI)* **2018**, *38*, 2162–2914. [CrossRef]
32. Karatuna, O. Quality Assurance in Antimicrobial Susceptibility Testing. In *Latest Research into Quality Control*; IntechOpen: London, UK, 2012. [CrossRef] [PubMed]
33. Arciola, C.R.; Campoccia, D.; Montanaro, L. Implant Infections: Adhesion, Biofilm Formation and Immune Evasion. *Nat. Rev. Microbiol.* **2018**, *16*, 397–409. [CrossRef] [PubMed]
34. Zhang, Y.; Dai, Z.; Li, X.; He, A.; Zheng, J.; Ding, M.; Li, Q.; Mou, Y.; Yang, D.; Xiu, W.; et al. Emerging Non-Antibiotic Strategies for Implant-Associated Biofilm Infections by Reprogramming the Dysregulated Immune Microenvironment. *npj Biofilms Microbiomes* **2026**, *12*, 42. [CrossRef] [PubMed]
35. Hall, D.C.; Palmer, P.; Ji, H.F.; Ehrlich, G.D.; Król, J.E. Bacterial Biofilm Growth on 3D-Printed Materials. *Front. Microbiol.* **2021**, *12*, 646303. [CrossRef] [PubMed]
36. Russo, T.A.; Marr, C.M. Hypervirulent Klebsiella Pneumoniae. *Clin. Microbiol. Rev.* **2019**, *32*, e00001-19. [CrossRef] [PubMed]
37. Vuotto, C.; Longo, F.; Balice, M.P.; Donelli, G.; Varaldo, P.E. Antibiotic Resistance Related to Biofilm Formation in Klebsiella Pneumoniae. *Pathogens* **2014**, *3*, 743. [CrossRef] [PubMed]
38. Park, S.-M.; Park, J.-M.; Kim, S.-K.; Heo, S.; Koak, J. Flexural Strength of 3D-Printing Resin Materials for Provisional Fixed Dental Prostheses. *Materials* **2020**, *13*, 3970. [CrossRef] [PubMed]

39. Kadauw, A.A.A. Neural Network Optimization of Mechanical Properties of ABS-like Photopolymer Utilizing Stereolithography (SLA) 3D Printing. *J. Manuf. Mater. Process.* **2025**, *9*, 116. [CrossRef]
40. Pszczółkowski, B.; Zaborowska, M. Effect of Layer Exposure Time in SLA-LCD Printing on Surface Topography, Hardness and Chemical Structure of UV-Cured Photopolymer. *Lubricants* **2025**, *13*, 406. [CrossRef]
41. Bolat, Ç.; Salmaz, S. An Investigation on the Wear Properties of the Photocurable Components Produced by Additive Manufacturing for Dentistry Applications: Combined Influences of UV Exposure Time, Building Direction, and Sliding Loads. *Polym. Eng. Sci.* **2024**, *64*, 5940–5958. [CrossRef]
42. Miedzińska, D.; Gieleta, R.; Popławski, A. Experimental Study on Influence of Curing Time on Strength Behavior of Sla-Printed Samples Loaded with Different Strain Rates. *Materials* **2020**, *13*, 5825. [CrossRef] [PubMed]
43. Dikova, T.D.; Dzhendov, D.A.; Ivanov, D.; Bliznakova, K. Dimensional Accuracy and Surface Roughness of Polymeric Dental Bridges Produced by Different 3D Printing Processes. *Arch. Mater. Sci. Eng.* **2018**, *94*, 65–75. [CrossRef]
44. Shim, J.S.; Kim, J.-E.; Jeong, S.H.; Choi, Y.J.; Ryu, J.J. Printing Accuracy, Mechanical Properties, Surface Characteristics, and Microbial Adhesion of 3D-Printed Resins with Various Printing Orientations. *J. Prosthet. Dent.* **2020**, *124*, 468–475. [CrossRef] [PubMed]
45. Gad, M.M.; Fouda, S.M.; Abualsaud, R.; Alshahrani, F.A.; Al-Thobity, A.M.; Khan, S.Q.; Akhtar, S.; Ateeq, I.S.; Helal, M.A.; Al-Harbi, F.A. Strength and Surface Properties of a 3D-Printed Denture Base Polymer. *J. Prosthodont.* **2022**, *31*, 412–418. [CrossRef] [PubMed]
46. Kaurani, P.; Hindocha, A.D.; Jayasinghe, R.M.; Pai, U.Y.; Batra, K.; Price, C. Effect of Addition of Titanium Dioxide Nanoparticles on the Antimicrobial Properties, Surface Roughness and Surface Hardness of Polymethyl Methacrylate: A Systematic Review. *F1000Research* **2023**, *12*, 577. [CrossRef] [PubMed]
47. AlGhamdi, M.A.; Fouda, S.M.; Al-Dulaijan, Y.A.; Khan, S.Q.; El Zayat, M.; Al Munif, R.; Albazroun, Z.; Amer, F.H.; Al Ammary, A.T.; Mahrous, A.A.; et al. Nanocomposite 3D Printed Resins Containing Titanium Dioxide (TiO2) Nanoparticles: An in Vitro Analysis of Color, Hardness, and Surface Roughness Properties. *Front. Dent. Med.* **2025**, *6*, 1581461. [CrossRef] [PubMed]
48. Guo, J.; Bing, Z.; Yang, J.; Tsoi, J.K.H.; Wang, Y. Effect of Roughness and Acidic Medium on Wear Behavior of Dental Resin Composite. *BMC Oral Health* **2022**, *22*, 470. [CrossRef] [PubMed]
49. Imazato, S.; Russell, R.R.B.; McCabe, J.F. Antibacterial Activity of MDPB Polymer Incorporated in Dental Resin. *J. Dent.* **1995**, *23*, 177–181. [CrossRef] [PubMed]
50. Pal, A.; Altaf, N.; Mahmood, A.; Akbar, S.; Maher, N.; Kumar, N.; Zafar, M.S.; Murcia, L.; Oñate-Sánchez, R.E. Exploring the Variability in Antibacterial Testing of Resin Dental Composites among Investigators: A Narrative Review. *Microbiol. Res.* **2023**, *14*, 1736–1750. [CrossRef]
51. Delcour, A.H. Outer Membrane Permeability and Antibiotic Resistance. *Biochim. Biophys. Acta Proteins Proteom.* **2009**, *1794*, 808–816. [CrossRef] [PubMed]
52. Breijyeh, Z.; Jubeh, B.; Karaman, R. Resistance of Gram-Negative Bacteria to Current Antibacterial Agents and Approaches to Resolve It. *Molecules* **2020**, *25*, 1340. [CrossRef] [PubMed]
53. Flemming, H.C. EPS—Then and Now. *Microorganisms* **2016**, *4*, 41. [CrossRef] [PubMed]
54. Wang, W.; Zhu, S.; Zhang, G.; Wu, F.; Ban, J.; Wang, L. Antibacterial and Thermomechanical Properties of Experimental Dental Resins Containing Quaternary Ammonium Monomers with Two or Four Methacrylate Groups. *RSC Adv.* **2019**, *9*, 40681–40688. [CrossRef] [PubMed]
55. Aati, S.; Akram, Z.; Shrestha, B.; Patel, J.; Shih, B.; Shearston, K.; Ngo, H.; Fawzy, A. Effect of Post-Curing Light Exposure Time on the Physico–Mechanical Properties and Cytotoxicity of 3D-Printed Denture Base Material. *Dent. Mater.* **2022**, *38*, 57–67. [CrossRef] [PubMed]
56. Zhang, Q.; Weng, S.; Hamel, C.M.; Montgomery, S.M.; Wu, J.; Kuang, X.; Zhou, K.; Qi, H.J. Design for the Reduction of Volume Shrinkage-Induced Distortion in Digital Light Processing 3D Printing. *Extreme Mech. Lett.* **2021**, *48*, 101403. [CrossRef]
57. Hetzler, S.; Rehm, S.; Räther, S.; Rues, S.; Zenthöfer, A.; Rammelsberg, P.; Schwindling, F.S. Fracture Toughness, Work of Fracture and Hardness of 3D-Printed Denture Base Resins. *Materials* **2025**, *18*, 4338. [CrossRef] [PubMed]
58. Marin, E.; Mukai, M.; Boschetto, F.; Sunthar, T.P.M.; Adachi, T.; Zhu, W.; Rondinella, A.; Lanzutti, A.; Kanamura, N.; Yamamoto, T.; et al. Production of Antibacterial PMMA-Based Composites through Stereolithography. *Mater. Today Commun.* **2022**, *32*, 103943. [CrossRef]
59. Costerton, J.W.; Stewart, P.S.; Greenberg, E.P. Bacterial Biofilms: A Common Cause of Persistent Infections. *Science* **1999**, *284*, 1318–1322. [CrossRef] [PubMed]

Disclaimer/Publisher's Note: The statements, opinions and data contained in all publications are solely those of the individual author(s) and contributor(s) and not of MDPI and/or the editor(s). MDPI and/or the editor(s) disclaim responsibility for any injury to people or property resulting from any ideas, methods, instructions or products referred to in the content.